THE EUROPEAN
PHYSICAL JOURNAL
SPECIAL TOPICS

Regular Article

Oscillatory wavelet-patterns in complex data: mutual estimation of frequencies and energy dynamics

Margarita Simonyan[1,a], Anna Fisun[2,b], Galina Afanaseva[2,c], Oxana Glushkovskaya-Semyachkina[3,d], Inna Blokhina[3,e], Anton Selskii[1,3,f], Maksim Zhuravlev[3,4,g], and Anastasiya Runnova[1,4,h]

[1] Institute of Cardiological Research, Saratov State Medical University, Saratov 410005, Russia
[2] Department of Pathological Physiology named after Academician A. A. Bogomolets, Saratov State Medical University, Saratov 410005, Russia
[3] Laboratory of Smart Sleep, Saratov State University, Saratov 410012, Russia
[4] Center for Coordination of Fundamental Scientific Activities, National Medical Research Center for Therapy and Preventive Medicine, Moscow 101990, Russia

Abstract In this work, we propose a modification of the wavelet oscillatory pattern method for analyzing energy characteristics of oscillatory components in complex signals. The energy analysis of oscillatory wavelet patterns allows fast two-dimensional sorting of oscillatory components in frequency and power, thus allows for further statistical calculation of the observed technologies. Counting operations are simply realized on the base of parallel calculations. The presented technique could be used in studying the electrophysiological features of brain activity during animals sleep and awake. The method was used in investigations of brain's electrophysiological characteristics during sleep and awake in animals. We found out that standard energy analysis could determine NREM sleep and awake condition in rats with normal weight and obesity. However, calculation of energy characteristics of the ECoG patterns in animals of two groups demonstrate a significant transformation of electrophysiological signals oscillatory structure during NREM sleep and awake in rats with severe visceral obesity. We suppose the changes of these characteristics may be associated with shifts in homeostasis indicators due to animal obesity.

1 Introduction

Study of living systems signals from on the base of mathematical analysis based on objective assessments of oscillatory processes and dynamic systems have been very common in recent decades. The classical Fourier transform for estimating spectral components and specially adapted methods for working with biomedical signals—calculations of correlation functions [1, 2], entropy estimations [3, 4], recurrence relations [5, 6], functional connectivity [7, 8], etc.—are used as the main tools of mathematical analysis.

In recent years, researchers are interested in such fundamental features of signals produced by living systems as strong unsteadiness, noise and simultaneous registration of many oscillatory components of various nature [9, 10]. In other words, early studies paid attention to the search for stationary components and trends of their changes in processing such signals. The remaining studies, rapidly changing components were considered as noise and/or insignificant. In particular, methods of evoked potentials [11], estimates of desynchronization/synchronization of alpha-, beta- and other rhythms [12, 13], as well as, for example, detection of stable sleep stages [14, 15] are implemented to analyze the electrical activity of the brain. However, in recent years, the focus of attention in studying of biological systems has increasingly shifted to the rapid processes accompanying the background activity of such objects. This process is connected with the growing of computer's technology calculating abilities, and the applied development of mathematical methods for processing complex signals.

To different components features account, researchers often substitute the classic windowed Fourier transform

[a] e-mail: dr.m-simonyan@yandex.ru

[b] e-mail: fisa89'89@mail.ru

[c] e-mail: gafanaseva@yandex.ru

[d] e-mail: glushkovskaya@mail.ru

[e] e-mail: inna-474@yandex.ru

[f] e-mail: selskiiao@gmail.com

[g] e-mail: zhuravlevmo@gmail.com

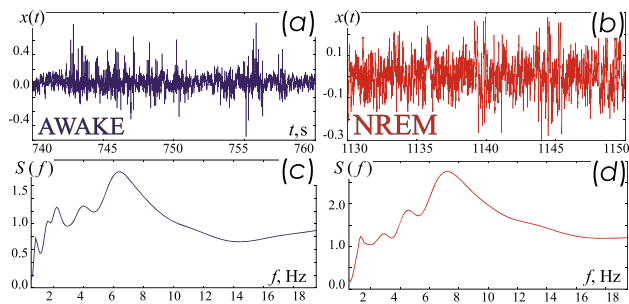[h] e-mail: a.e.runnova@gmail.com (corresponding author)

Fig. 1 The left panel corresponds to the rat's awake/REM sleep (AWAKE), the right panel corresponds to behavioral sleep (NREM), for both states, respectively, the following graphs are given: **a**, **b**—fragments of the ECoG signal recorded in rat #1; **c**, **d**—Furie-spectrum calculated for the corresponding ECoG signals

by the wavelet transformation. It is known that the use of harmonic functions as the parent basis, turns the continuous wavelet transformation into a windowed Fourier transformation, which makes possible the direct correlation of Fourier and wavelet spectra [16]. In general, the preference of the Fourier wavelet transformation to the spectrum is associated with the averaging properties of the Fourier transformation with respect to strong signal nonstationarity. In particular, Fig. 1 illustrates this fact and shows weak differences in the low-frequency region for ECoG recorded in the frontal regions of the rat brain during awake and NREM sleep. Figure 2 presents the time-frequency surfaces calculated on the basis of a continuous wavelet transformation from ECoG fragments

shown in Fig. 1. Analysis of Fig. 2 data distinguishes significantly greater differences in wavelet surfaces compared with Fourier spectra. In particular, in NREM sleep, ECoG activity becomes less homogeneous with expressed powerful energy spikes of oscillation components in the considered frequency intervals Δf.

To analyze biomedical signals, various basic functions of continuous wavelet transformation are used, in particular, the Morlet, MHAT or Paul wavelet [17, 18]. Based on the continuous wavelet transformation, in our work Runnova, et al. [19] a method for constructing and evaluating oscillatory patterns was implemented—various components that coexist at each moment in the recorded electroencephalography (EEG) or electrocorticograms (ECoG). We "deploy" each one-dimensional signal in the time-frequency plane, on which we further allocate an oscillatory component, for which we can estimate the average frequency and lifetime. By choosing a number of interested frequency ranges, we can calculate the statistical oscillatory characteristics of a living system, namely, the average number and lifetime of oscillatory components in a particular frequency range. In this work, we develop the proposed approach by introducing the energy weight of each oscillation component into consideration. We use the proposed method to evaluate a small experimental material based on the analysis of invasive ECoG in Wistar rats recorded in two homogeneous groups of males, divided by their weight characteristics.
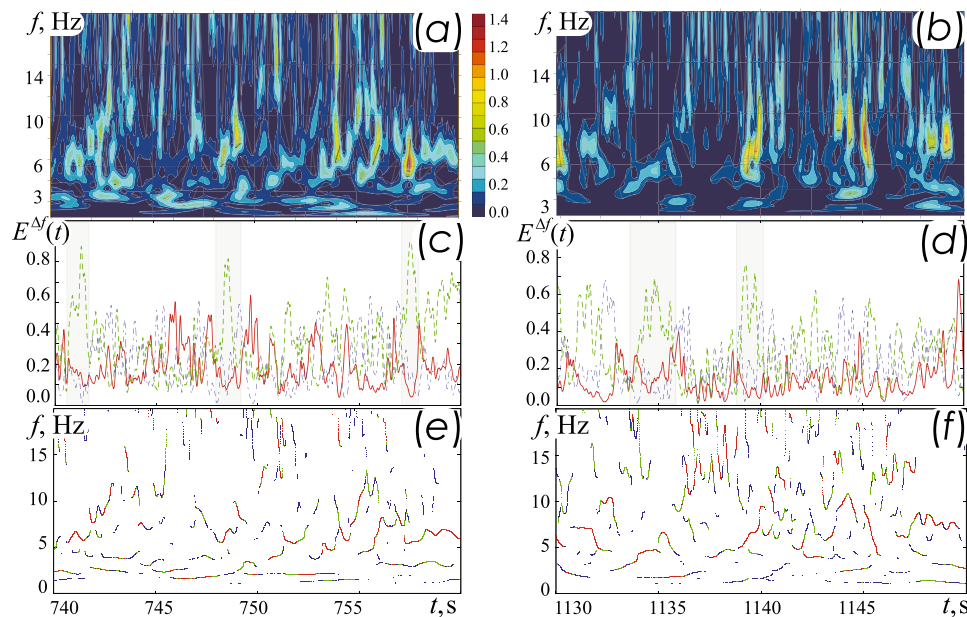

Fig. 2 The left and right panels correspond to the rat's physiological states, awake and NREM-sleep, respectively. **a**, **b**—wavelet spectrums $CWT(f, t)$; **c**, **d** are the energy estimations $E^{\Delta f}(t) = CWT^2(f, t)$ calculated for the frequency ranges $\Delta f = [5; 10]$ (solid red line), $\Delta f = [3; 5]$ (green dashed line), $\Delta f = [1; 2.5]$ (blue thin dashed line); **e**, **f**—constructions of the skeleton characteristics, characterizing the maximum values of $CWT(f, t)$, the first skeletons corresponding to the highest values are highlighted in red, the second-largest in green and the third in blue

2 Method for assessing energy oscillatory components (patterns)

The mathematical basis of the oscillatory patterns method is the continuous wavelet transformation (CWT) [20–22]:

$$W(s,t) = \sqrt{s} \int_{-\infty}^{\infty} x(t)\psi^* \left(\frac{t-t_0}{s} \right) dt, \qquad (1)$$

where $x(t)$ is the analyzed signal, and s is the time scale that determines the wavelet width, "*" is the complex conjugation, and $\psi_{t_0,s}(t)$ is the basis of the wavelet transform in the form of a complex function. In the framework of working with biological signals, a Morlet wavelet [22] is used frequently:

$$\psi_{t_0,s}(t) = \sqrt{f}\pi^{\frac{1}{4}} e^{j\omega_0 f(t-t_0)} e^{\frac{f(t-t_0)^2}{2}}, \qquad (2)$$

where $\omega_0 = 2\pi$ is the wavelet scaling parameter that provides a relationship between the time scale of the wavelet transform (s) and the Fourier transform frequency (f), where $f = 1/s$. Thus, we can use with the usual classical frequency representation of signals when calculating CWT.

In the framework of applying CWT, in particular, the skeleton CWT method [21, 23, 24] is used to improve the quality of assessment of such coexisting processes. This technique is based on the identification in the analyzed frequency range of the local maximum in the instantaneous distribution of CWT energy at every time. The following relation determines the instant CWT-energy distribution:

$$E(f, t_0) = W(f, t_0)^2. \qquad (3)$$

Figure 2e, f illustrates the classical skeleton method, according to which a set of local extrema of function (3), can be identified for each time moment t_0. The method of oscillatory patterns estimation is based on a special sorting of local extrema data, i.e., skeletons.

Firstly, in each time moment t_n, we compose a set of frequencies f_j, where $j = 1, 2, \ldots, m$, which correspond to the local maximum $E(f_j, t_n)$ (3). Here, the sequence number j characterizes only the sequence number of the extrema and is not related to the amplitude $E(f_j, t_n)$. However, information about the value $E(f_j, t_n)$ is stored for each point (f_j, t_n). Thus, in the process of analyzing the total duration of the studied signal, a set of frequencies f_j^n is formed, where n is the duration of the experimental signal, i.e., the number of time samples in the signal.

Secondly, we denote the condition for the development of an activity pattern with a frequency f_j. To do this, we consider the following condition on each time interval $[t_n; t_{n+1}]$ for each frequency f_j:

$$\sqrt{(f_j^n - f_s^{n+1})^2} < \delta, \qquad (4)$$

where f_j^n is a set of frequencies for which the local maximum $E(f_j, t_n)$ (3) observed at time step t_n, and f_j^{n+1} are similar set of frequencies with local maximum $E(f_j, t_{n+1})$ for the next time step t_{n+1}, δ is a numerical constant. The choice of the value of δ-constant is based on the signal sampling frequency and exceeds it by 1–2 orders of magnitude, which allows minimizing the loss of information about the frequency patterns existing in the signal under study and reducing the influence of the signal's numerical noise.

Next, we test a condition (4). If condition (4) is satisfied for some frequencies $f_{(a1)^n}$ and $f_{(a2)^{n+1}}$, then the activity at these frequencies in the time interval $[t_n; t_{n+1}]$ can be regarded as the development of one oscillatory pattern. We then denote the frequency data $f_{(a1)^n}$ and $f_{(a2)^{n+1}}$ as $(a1)$ and $(a2)$, respectively. Next, for frequency $(a2)$, we again analyze (4) for the next time step t_{n+2}. If the condition is satisfied for a given time step, then the identified pattern will continue further with a certain frequency $(a3)$.

The described actions must be repeated cyclically until the moment when condition (4) becomes incorrect, in other words, until the end of the activity of this oscillatory pattern. Thus, each oscillatory pattern P can be described by the frequency at each time moment of its existence, i.e., $P(f, t) = \{\{(a1), t_n\}, \{(a2), t_{n+1}\}, \ldots, \{(am), t_{n+m}\}\}$, where m characterizes the time duration of pattern "life." Then the time duration T of the pattern P can be defined as

$$T = t_{n+m} - t_n, \qquad (5)$$

and for the case of equidistant experimental time series, we use the expression $T = m\Delta t$, where Δt is the sampling time interval. So, the average frequency f_{md} can be estimated for each frequency pattern P as

$$f_{md} = \sum_{i=1}^{m} (ai)/m. \qquad (6)$$

For further analysis, we denote the following selection criterion for the correct oscillatory patterns P. If the time duration τ of the pattern P does not exceed the oscillation period of its average frequency f_{md}, i.e., $\tau < (f_{md})^{-1}$, then this pattern must be considered a random noise interference and should not be taken into account in the further analysis of the signal. This method was proposed and tested earlier, in the our works [19, 25].

We propose to expand this approach by supplementing it with an estimate of the energy of each P oscillatory pattern. To do this, we return to the stored energy value $E_{i,j}$ for each point (f_i, t_j) representing part of the detected patterns P. At each time t_j we form an array of all energy values $\{E_{1,j}, \ldots, E_{k,j}, \ldots\}$, where $k = 1, \ldots, r$, and r is the number of frequencies observed for time t_j on the computed pattern surface P. In the array $\{E_{1,j}, \ldots, E_{k,j}, \ldots, E_{r,j}\}$ we estimate the maximum energy value $E_{\max,j}$, $E_{\max,j} > E_{k,j}$, for

Fig. 3 The top **a**, **b** and bottom **c**, **d** panels correspond to the CWT-estimation of energetic oscillatory patterns, calculated in groups I and II, respectively. The left diagrams show the results of the assessment of ECoG fragments of active wakefulness in rats, and the right diagrams show NREM sleep. The color of the patterns corresponds to the value of the normalized energy, according to the scale below
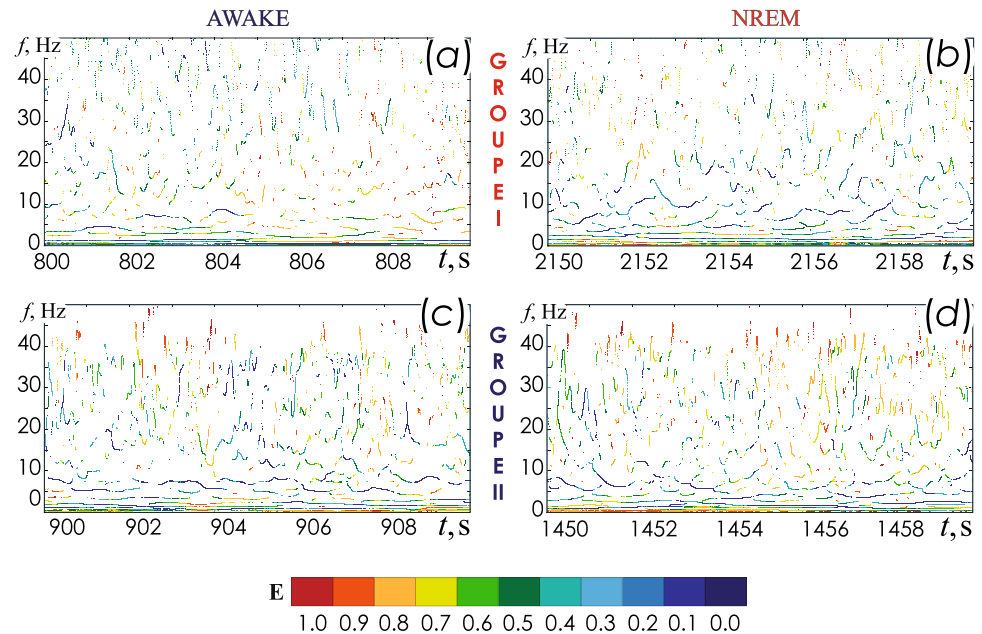
$\forall k$. And we normalize energy values as:

$$\{\langle E_{1,j}\rangle, \ldots, \langle E_{k,j}\rangle, \ldots, \langle E_{r,j}\rangle\}$$
$$= \left\{\frac{E_{1,j}}{E_{\max,j}}, \ldots, \frac{E_{k,j}}{E_{\max,j}}, \ldots, \frac{E_{r,j}}{E_{\max,j}}\right\}. \quad (7)$$

Normalization is performed separately for each moment j of time, which allows use standard parallel mode for program realization of this algorithm.

Next, we again return to the sorting of patterns P, and for all points $(f, t)_p$, constituting one pattern P with duration m, we calculate the average energy characteristic E of the pattern as

$$E = \frac{\sum_{p=1}^{m}\langle E(f,t)_p\rangle}{m}. \quad (8)$$

Therefore, each pattern is described by three characteristics: mean frequency f_{md}, duration or lifetime T, mean energy E. We demonstrate the results of the proposed method in processing on an ECoG fragment. Figure 3 shows the results using the energetic patterns method. Each pattern on the $(f; t)$ plane is colored according to its average energy E.

Figure 3b allows us to see that the oscillatory activity dynamically develops over time and formes oscillatory patterns with various durations, changing in the frequency and amplitude zones, up to complete destruction. Obviously, the our exstension of the wavelet-technique used to process the ECoGs as a whole has outstanding sensitivity and allows identifying activity of a very low magnitude. In this situation, a rational analysis of the evolution of the entire frequency spectrum is adopted to gain a detailed understanding of signal oscillatory structure. We can observe patterns of oscillatory activity of fluctuating amplitude in different frequency bands. Moreover, the using of this method allows for a simple quantitative assessment of signal patterns for a specific frequency range, or time interval, or energy diapason.

Figure 3b allows us to see that the oscillatory activity dynamically develops over time and formes oscillatory patterns with various durations, changing in the frequency and amplitude zones, up to complete destruction. Obviously, the our exstension of the wavelet-technique used to process the ECoGs as a whole has outstanding sensitivity and allows identifying activity of a very low magnitude. In this situation, a rational analysis of the evolution of the entire frequency spectrum is adopted to gain a detailed understanding of signal oscillatory structure. We can observe patterns of oscillatory activity of fluctuating amplitude in different frequency bands. Moreover, the using of this method allows for a simple quantitative assessment of signal patterns for a specific frequency range, or time interval, or energy diapason.

3 Approbation of the method on experimental data of electrocorticograms of Wistar rats

3.1 Animals

Experiments were performed in 18 male Wistar rats at the biological laboratory of Saratov State University (Saratov, Russia). The living conditions and experimental work in animals followed the recommendations in the ARRIVE guidelines 2.0 [26], were done in accordance with "the Guide for the Care and Use of Laboratory Animals" and local ethical guidelines, and it was approved by the Local Bioethics Commission of

the Saratov State University. Animals were kept in a vivarium at temperature of $22 \pm 2°$ C and humidity of 40–60% with 12-h day cycle (artificial illumination mode). Experimental animals were divide into two groups in three-months age. The first group (5 males) were kept on a standard diet with a total calorie content of 270 kcal/100 g (20% protein; 40% carbohydrates; 40% fat of total calories). The second group (13 males) had a high-calorie diet of about 500 kcal/100 g (20% protein; 70% carbohydrates; 10% fat of total calories). For purpose of modeling of real conditions, the animals had unlimited access to food and drinking water.

At the age of 5 months rats were implanted with epidural electrodes for ECoG recording. Pinnacle Technology (Taiwan) was used to record two-channels ECoG. During stereotaxic operation, rats were kept under inhalation anesthesia (2% isoflurane at 1 L/min $N_2O:O_2$—70:30) and were implanted with two silver electrodes (tip diameter 2–3 mm) at a depth of 150 mm inserted in right/left frontal cortex (L: 2.5 mm and D: 2 mm from bregma). Small burr holes were drilled in the scull, ECoG wire leads were inserted in the epidural space and secured with dental acrylic. In order to control postoperative pain, Ibuprofen (15 mg/kg) was provided in drinking water during 2–3 days prior to surgery and more than 3 days after the surgery. Rats were allowed 10 days to recover from surgery prior to recording session. ECoG was recorded during the whole day in animals' free state, for each rat.

The first group is characterized by standard animals weight (400–480 g), in the second group, the weight of rats ranged from 645 to 740 g, which corresponds to significant differences according to the Wilcoxon test ($p < 0.05$). The body length of the animals in both groups coincided and was in the range of 27–30 cm.

3.2 Methods

Two stages of the sleep-wake cycle were identified in ECoG: NREM-sleep and wakefulness/REM-sleep. The state of Wake/REM sleep (Fig. 1a) and NREM-sleep (Fig. 1b) were detected automatically using wavelet-based algorithm described elsewhere [27, 28]. This methodology is based on the assessment of (1) classic energy of CWT in different ranges of ECoG signals and (2) individually calculated NREM-sleep start/end thresholds for each rat.

Oscillation patterns and their main characteristics (average frequency f_{md}, duration T and average energy E) were calculated for each ECoG record. Statistical analysis was carried out for two distinguished physiological states within the following frequency ranges: Δf_1 [0.1; 5] Hz, Δf_2 [14; 16] Hz, Δf_3 [25; 35] Hz, Δf_4 [40; 50] Hz. For each frequency range, the number of patterns N was counted and the average characteristics of the lifetime T, energy E of the pattern with an average frequency falling within the given frequency range were estimated.

Mean, median, and standard deviation were used in descriptive statistics of the data. The Mann–Whitney U test for independent samples was used for the comparison of quantitative data [29]. The results with a p value ≤ 0.001 were considered statistically significant. Statistical analyses were performed using the SPSS version 22.0 software for Windows (IBM, Armonk, NY, USA).

4 Results

The analysis of the duration of sleep episodes per day showed no significant differences for the two groups of animals; the total duration of sleep periods was [31; 40]% for all rats. The number of sleep episodes varied within [3; 10] during the day, naturally increasing during the daylight period.

The results of statistical analysis of oscillatory patterns in the frequency ranges under consideration are shown in Figs. 4 and 5. The distribution of the number, lifetime, and energy of patterns during the NREM sleep and awake states are represent for each animal. We observe variegated dynamics for the considered characteristics of oscillatory patterns in different frequency ranges. However, in general, it should be noted that in group II, all characteristics of oscillatory patterns demonstrate almost identical dynamics during sleep and wakefulness. Such dynamics is not typical for normal weight animals signals recording (group I).

For the low-frequency range Δf_1, observed a decrease in the number and an increase in the lifetime of patterns in animals of the second group, highlighted in red in the diagrams in Fig. 4a. The energy characteristics show a large scatter and do not differ quantitatively. At the same time, for each animal from group II for states of sleep and wakefulness, their values, as before, do not differ significantly.

In the Δf_2 range, the number and lifetime of patterns in animals of group II increase (Fig. 4b) compared to animals with normal weight. The mean energy characteristics E of the oscillational structures still do not differ.

The Δf_3 range is characterized by an increase in the number N and lifetime T of patterns, similar to the Δf_2 range, as shown in Fig. 5a. The rat #11 shows differences in the mean energy E during sleep and wakefulness. At the same time, we observed no differences between the two groups in the mean energy levels E.

The characteristics of the "fastest" oscillatory patterns are shown in Fig. 5b. We observed no significant differences between the two groups in the lifetime T of the patterns at high activity frequencies in the Δf_4 range. However, the number N and energy E of patterns differ significantly in groups I and II. In addition, in group II, 5 animals (#6–#10) demonstrate a very homogeneous dynamics of the energy characteristics of the oscillatory structure during sleep and wakefulness.

600

Eur. Phys. J. Spec. Top. (2023) 232:595–603

Fig. 4 The diagrams of pattern's numbers N, duration T and energy E in ranges Δf_1 (**a**) and Δf_2 (**b**) in two rat's groups. The diagrams depict the following statistical characteristics of numerical indicators: the first and the third quartiles (25–75%, inside the box); the median and the mean (transverse line and point inside the box, respectively); 1.5 interquartile range (shown by whiskers); and outliers represented by asterisks. Blue color indicate characteristics for wakefulness, red color indicate NREM sleep. Animal numbers are given on each diagram, animal groups are highlighted in green (Group I) and red (Group II)
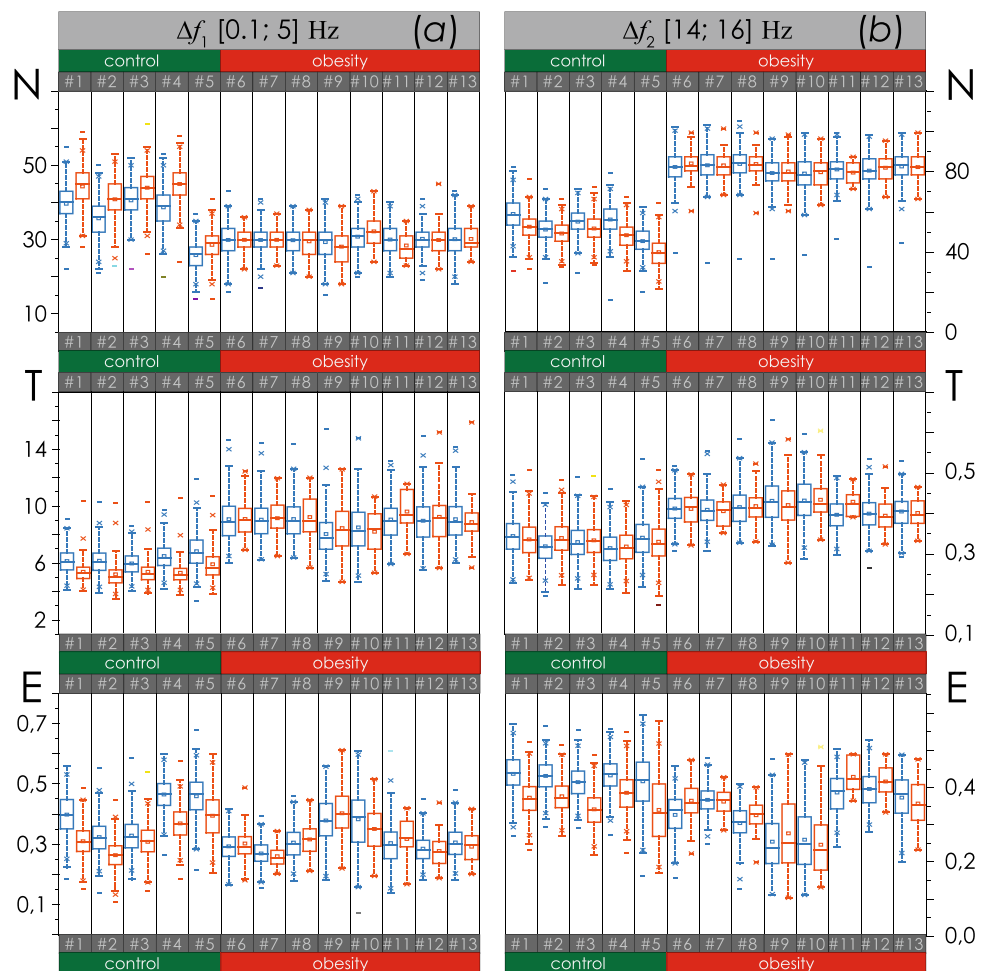

5 Discussion

The proposed modification of the previously developed method for estimating oscillatory patterns based on a continuous wavelet transformation allows, as before, identifying the individual oscillatory components of the signal for each frequency interval. In addition to these possibilities, a new energy characteristic appears. During the testing performed on experimental ECoG, we used a variant of calculating the characteristic E, normalized for each frequency interval. Thus, we independently assessed the dynamics of oscillatory activity within each frequency interval.

Another modification of the numerical estimate of the energy of oscillatory wavelet patterns with normalization in a certain time interval is possible. In this case, automatic allocation of the the most energetically significant ranges during the required time intervals becomes possible. This approach seems to be more important in solving the problems of psychophysiology arising from the analysis of human cognitive processes. In particular, some studies demonstrate the connection of short-term periods of alpha and delta activity in the EEG with the long-term maintenance of a consistently high level of active human attention [9, 12, 13, 30, 31].

The use of the proposed modification of the wavelet analysis will allow obtaining a detailed assessment of the presence and energy value of oscillational activity in low- and high-frequency activity. Further statistical analysis of the different EEG rhythms detected in this way can provide additional information about the possible correlation of such patterns and attentional decrease. Such studies are in demand in technologies for controlling loss of control, for example, during prolonged driving [32], as well as in the development of brain–computer interface [33].

Regarding the completed approbation of the presented technique, we can note that today in the scientific community rats are recognized as a biological model of human obesity [34, 35]. The approach of animals feeding in the second group used in this work corresponds to the induction of obesity based on a high-carbohydrate diet [36–38]. The speed of obesity development with such a diet is lower compared with the high-fat diet, in which the fat content ranges from 30–40 to 60% of the total energy value of the diet [39, 40]. At the same time, obesity developing in this diet seems to be the best model of visceral obesity in humans according to [36, 41]. At the same time, this type of obesity

Fig. 5 The diagrams of pattern's numbers N, duration T and energy E in ranges Δf_3 (**a**) and Δf_4 (**b**) in two rat's groups. The diagrams depict the following statistical characteristics of numerical indicators: the first and the third quartiles (25–75%, inside the box); the median and the mean (transverse line and point inside the box, respectively); 1.5 interquartile range (shown by whiskers); and outliers represented by asterisks. Blue color indicate characteristics for wakefulness, red color indicate NREM sleep. Animal numbers are given on each diagram, animal groups are highlighted in green (Group I) and red (Group II)
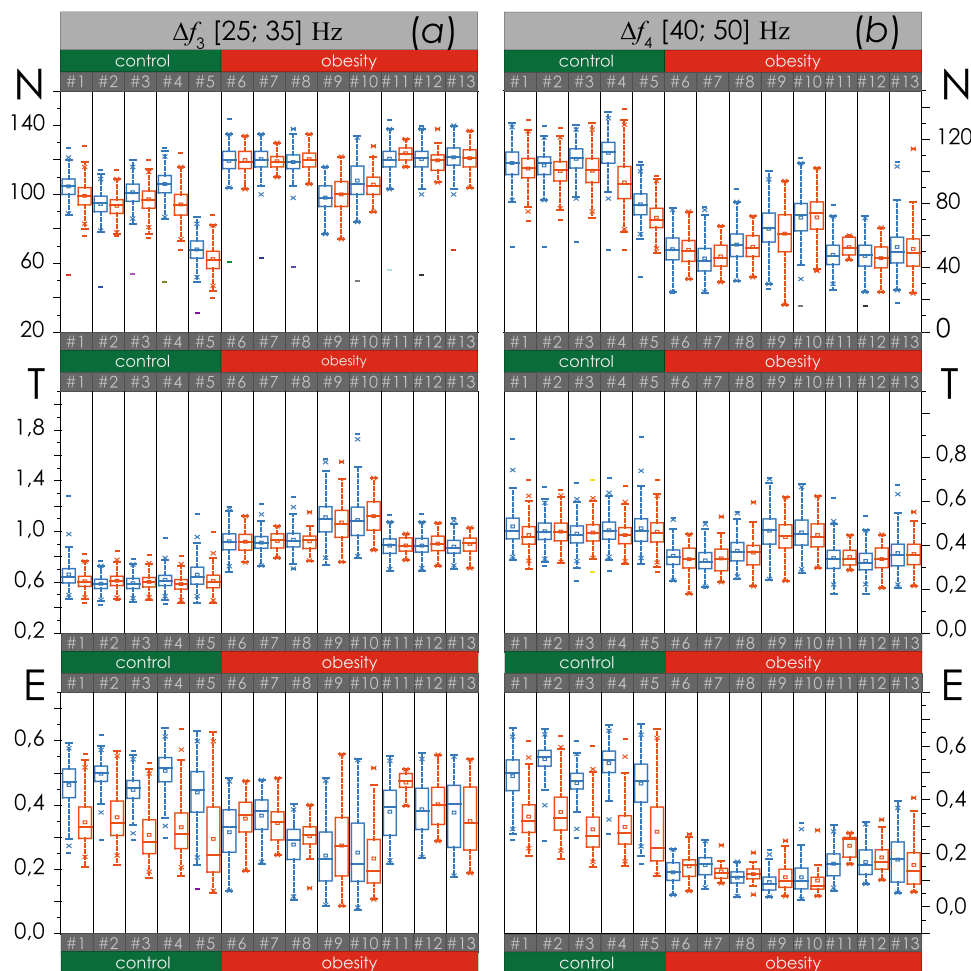
apparently plays a great role as a global factor of cardiovascular risk among the various patients classes of population in modern developed countries [42–44]. Changes in the functioning of the cardiovascular system and an increase in the load on it lead to disturbances in the normal nutrition of the most energy-consuming organ—the brain. However, at the same time, an increase in the percentage of adipose tissue in the body leads both to chronic inflammatory processes and to development of neurodegenerative disorders.

In our work, we show a change in the structure of brain activity that develops in obese rats based on the method of energy oscillatory patterns. A conditionally "rough" energy assessment of ECoG signals performed during the detection of sleep and awake states in entire frequency ranges [27, 28] demonstrated identical oscillatory dynamics of ECoG in rats of groups I and II. In other words, as for the classical frequency analysis, the states of sleep and awake in obesity are close to the same physiological states in animals with normal weight. At the same time, pattern analysis demonstrates very significant changes in the internal structure of oscillatory dynamics. At low frequencies, changes affect mainly the number and lifetime of patterns, and at high frequencies, they also greatly change the level of expression,

i.e., the energy of the oscillational components. In addition, the question of the specific physiological causes of these changes in electrophysiological activity remains open and requires further explaining studies.

6 Conclusion

We provide an additional modification of spectral analysis based on continuous wavelet transform. The proposed estimation of the oscillatory components existing on a two-dimensional time-frequency plane calculated on the base of the wavelet transformation on a one-dimensional signal makes possible the expansion of the possibilities to evaluate the properties of signals. This technique is suggested for biomedical signals, but can also be adapted to solve radiophysical problems, for example, in developing complex algorithms for encrypting/decrypting signals of a wide spectrum.

Declarations

Conflict of interest All authors declare that they have no conflicts of interest.

References

1. A.S. Karavaev, A.S. Borovik, E.I. Borovkova, E.A. Orlova, M.A. Simonyan, V.I. Ponomarenko, V.V. Skazkina, V.I. Gridnev, B.P. Bezruchko, M.D. Prokhorov et al., Low-frequency component of photoplethysmogram reflects the autonomic control of blood pressure. Biophys. J. **120**(13), 2657–2664 (2021)
2. C. Metzner, A. Schilling, M. Traxdorf, H. Schulze, P. Krauss, Sleep as a random walk: a super-statistical analysis of eeg data across sleep stages. Commun. Biol. **4**(1), 1–11 (2021)
3. D. Parbat, M. Chakraborty, A novel methodology to study the cognitive load induced eeg complexity changes: Chaos, fractal and entropy based approach. Biomed. Signal Process. Control **64**, 102277 (2021)
4. J. Lerga, N. Saulig, L. Stanković, D. Seršić, Rule-based EEG classifier utilizing local entropy of time-frequency distributions. Mathematics **9**(4), 451 (2021). https://doi.org/10.3390/math9040451
5. R.A. Jaswal, S. Dhingra, J.D. Kumar, Designing multimodal cognitive model of emotion recognition using voice and EEG signal, in *Recent Trends in Electronics and Communication* (Springer, London, 2022), pp. 581–592
6. A. Runnova, A. Selskii, E. Emelyanova, M. Zhuravlev, M. Popova, A. Kiselev, R. Shamionov, Modification of joint recurrence quantification analysis (JRQA) for assessing individual characteristics from short EEG time series. Chaos Interdiscip. J. Nonlinear Sci. **31**(9), 093116 (2021)
7. A.J. Mackintosh, R. de Bock, Z. Lim, V.-N. Trulley, A. Schmidt, S. Borgwardt, C. Andreou, Psychotic disorders, dopaminergic agents and EEG/MEG resting-state functional connectivity: a systematic review. Neurosci. Biobehav. Rev. **120**, 354–371 (2021)
8. T. Talukdar, A. Nikolaidis, C.E. Zwilling, E.J. Paul, C.H. Hillman, N.J. Cohen, A.F. Kramer, A.K. Barbey, Aerobic fitness explains individual differences in the functional brain connectome of healthy young adults. Cerebral Cortex **28**, 1–10 (2017)
9. Z. Dai, J. De Souza, J. Lim, P.M. Ho, Y. Chen, J. Li, N. Thakor, A. Bezerianos, Y. Sun, EEG cortical connectivity analysis of working memory reveals topological reorganization in theta and alpha bands. Front. Hum. Neurosci. **11**, 237 (2017)
10. U. Braun, A. Schäfer, H. Walter, S. Erk, N. Romanczuk-Seiferth, L. Haddad, J.I. Schweiger, O. Grimm, A. Heinz, H. Tost et al., Dynamic reconfiguration of frontal brain networks during executive cognition in humans. Proc. Natl. Acad. Sci. **112**(37), 11678–11683 (2015)
11. B. Schöne, T. Gruber, S. Graetz, M. Bernhof, P. Malinowski, Mindful breath awareness meditation facilitates efficiency gains in brain networks: a steady-state visually evoked potentials study. Sci. Rep. **8**(1), 1–10 (2018)
12. A. Runnova, A. Selskii, A. Kiselev, R. Shamionov, R. Parsamyan, M. Zhuravlev, Changes in EEG alpha activity during attention control in patients: association with sleep disorders. J. Personal. Med. **11**(7), 601 (2021)
13. A.D. Nordin, W.D. Hairston, D.P. Ferris, Faster gait speeds reduce alpha and beta EEG spectral power from human sensorimotor cortex. IEEE Trans. Biomed. Eng. **67**(3), 842–853 (2019)
14. S. Shustak, L. Inzelberg, S. Steinberg, D. Rand, M.D. Pur, I. Hillel, S. Katzav, F. Fahoum, M. De Vos, A. Mirelman et al., Home monitoring of sleep with a temporary-tattoo EEG, EOG and EMG electrode array: a feasibility study. J. Neural Eng. **16**(2), 026024 (2019)
15. P. Pearl, J. Beal, M. Eisermann, S. Misra, P. Plouin, S. Moshe, J. Riviello, D. Nordli, E. Mizrahi, Normal EEG in wakefulness and sleep, preterm, term, infant, adolescent, in *Niedermeyer's Electroecephalography: Basic Principles, Clinical Applications, and Related Fields*, 7th edn (Oxford University Press, Oxford, 2018)
16. M. Sifuzzaman, M.R. Islam, M.Z. Ali, Application of wavelet transform and its advantages compared to Fourier transform. J. Phys. Sci. **13**(1), 121–134 (2009)
17. A. Cohen, Wavelet methods in numerical analysis. Handb. Numer. Anal. **7**, 417–711 (2000)
18. P. Bhatia, J. Boudy, R. Andreão, Wavelet transformation and pre-selection of mother wavelets for ECG signal processing, in *Proceedings of the 24th IASTED International Conference on Biomedical Engineering* (2006) pp. 390–395
19. A. Runnova, M. Zhuravlev, R. Ukolov, I. Blokhina, A. Dubrovski, N. Lezhnev, E. Sitnikova, E. Saranceva, A. Kiselev, A. Karavaev et al., Modified wavelet analysis of ECoG-pattern as promising tool for detection of the blood-brain barrier leakage. Sci. Rep. **11**(1), 1–8 (2021)
20. B. Torresani, *Continuous Wavelet Transform*, vol. 675 (Savoire, Paris, 1995), p.676
21. A.E. Hramov, A.A. Koronovskii, V.A. Makarov, A.N. Pavlov, E. Sitnikova, *Wavelets in Neuroscience* (Springer, London, 2015)
22. A.N. Pavlov, A.E. Hramov, A.A. Koronovskii, E.Y. Sitnikova, V.A. Makarov, A.A. Ovchinnikov, Wavelet analysis in neurodynamics. Phys. Usp. **55**(9), 845 (2012)
23. E. Sitnikova, A.E. Hramov, V. Grubov, A.A. Koronovsky, Age-dependent increase of absence seizures and intrinsic frequency dynamics of sleep spindles in rats. Neurosci. J. **2014** (2014)
24. E. Sitnikova, A.E. Hramov, V. Grubov, A. A. Koronovsky, Time-frequency characteristics and dynamics of sleep spindles in WAG/Rij rats with absence epilepsy. Brain research. 1543, 290-299 (2014)
25. K. Sergeev, A. Runnova, M. Zhuravlev, O. Kolokolov, N. Akimova, A. Kiselev, A. Titova, A. Slepnev, N.

Semenova, T. Penzel, Wavelet skeletons in sleep EEG-monitoring as biomarkers of early diagnostics of mild cognitive impairment. Chaos Interdiscip. J. Nonlinear Sci. **31**(7), 073110 (2021)

26. N. Percie du Sert, A. Ahluwalia, S. Alam, M.T. Avey, M. Baker, W.J. Browne, A. Clark, I.C. Cuthill, U. Dirnagl, M. Emerson et al., Reporting animal research: explanation and elaboration for the ARRIVE guidelines 2.0. PLoS Biol. **18**(7), 3000411 (2020)

27. M. Zhuravlev, A. Runnova, K. Smirnov, E. Sitnikova, Spike-wave seizures, NREM sleep and micro-arousals in WAG/Rij rats with genetic predisposition to absence epilepsy: developmental aspects. Life **12**(4), 576 (2022)

28. A. Runnova, M. Zhuravlev, A. Kiselev, R. Ukolov, K. Smirnov, A. Karavaev, E. Sitnikova, Automatic wavelet-based assessment of behavioral sleep using multichannel electrocorticography in rats. Sleep Breath. **25**(4), 2251–2258 (2021)

29. R.F. Woolson, W.R. Clarke, *Statistical Methods for the Analysis of Biomedical Data* (Wiley, New York, 2011)

30. S.W. Hughes, V. Crunelli, Thalamic mechanisms of EEG alpha rhythms and their pathological implications. Neuroscientist **11**(4), 357–372 (2005)

31. V.V. Makarov, M.O. Zhuravlev, A.E. Runnova, P. Protasov, V.A. Maksimenko, N.S. Frolov, A.N. Pisarchik, A.E. Hramov, Betweenness centrality in multiplex brain network during mental task evaluation. Phys. Rev. E **98**(6), 062413 (2018)

32. T. Tuncer, S. Dogan, A. Subasi, EEG-based driving fatigue detection using multilevel feature extraction and iterative hybrid feature selection. Biomed. Signal Process. Control **68**, 102591 (2021)

33. B. Venkata Phanikrishna, P. Pławiak, A. Jaya Prakash, A brief review on EEG signal pre-processing techniques for real-time brain-computer interface applications (2021)

34. J.R. Speakman, *Use of High-Fat Diets to Study Rodent Obesity as a Model of Human Obesity* (Nature Publishing Group, Berlin, 2019)

35. K. Kanasaki, D. Koya, Biology of obesity: lessons from animal models of obesity. J. Biomed. Biotechnol. **2011** (2011)

36. V. Von Diemen, E.N. Trindade, M.R.M. Trindade, Experimental model to induce obesity in rats. Acta Cirurgica Brasileira **21**, 425–429 (2006)

37. L. Thibault, Chapter 13—animal models of dietary-induced obesity, in *Animal Models for the Study of Human Disease*. ed. by P.M. Conn (Academic Press, Boston, 2013), pp.277–303

38. S.K. Panchal, H. Poudyal, A. Iyer, R. Nazer, A. Alam, V. Diwan, K. Kauter, C. Sernia, F. Campbell, L. Ward et al., High-carbohydrate, high-fat diet-induced metabolic syndrome and cardiovascular remodeling in rats. J. Cardiovasc. Pharmacol. **57**(5), 611–624 (2011)

39. H.-J. Kim, S. Kim, A.Y. Lee, Y. Jang, O. Davaadamdin, S.-H. Hong, J.S. Kim, M.-H. Cho, The effects of gymnema sylvestre in high-fat diet-induced metabolic disorders. Am. J. Chin. Med. **45**(04), 813–832 (2017)

40. A.M. Stranahan, Models and mechanisms for hippocampal dysfunction in obesity and diabetes. Neuroscience **309**, 125–139 (2015)

41. R.K. Bains, S.E. Wells, D.M. Flavell, K.M. Fairhall, M. Strom, P. Le Tissier, I.C. Robinson, Visceral obesity without insulin resistance in late-onset obesity rats. Endocrinology **145**(6), 2666–2679 (2004)

42. A. Tchernof, J.-P. Després, Pathophysiology of human visceral obesity: an update. Physiol. Rev. (2013)

43. M.-È. Piché, S.J. Weisnagel, L. Corneau, A. Nadeau, J. Bergeron, S. Lemieux, Contribution of abdominal visceral obesity and insulin resistance to the cardiovascular risk profile of postmenopausal women. Diabetes **54**(3), 770–777 (2005)

44. G.A. Chumakova, T.Y. Kuznetsova, M.A. Druzhilov, N.G. Veselovskaya, Visceral adiposity as a global factor of cardiovascular risk (in rus.). Russ. J. Cardiol. **5**, 7–14 (2018)